

Multi-century tree-ring reconstruction of annual streamflow for the Maule watershed, South-Central Chile



R. Urrutia, A. Lara, R. Villalba, C. Le Quesne & A. Cuq
Laboratorio de Dendrocronología, Instituto de Silvicultura, Facultad de Ciencias Forestales, Universidad Austral de Chile, Valdivia, Chile (rociourrutia@uach.cl)



1. Introduction

Water availability has been recognized as one of the main limitations for future economic development for extensive regions of the world (Arnell et al. 2001; Viviroli et al. 2003). This can even be applied to areas with relatively high amounts of precipitation, such as the valdivian rainforest eco-region in Chile and Argentina (35° – 48° S, Lara et al., 2008).

Streamflow and water availability are essential for irrigation, human consumption and hydropower generation which accounts for 50% of the total Chilean electrical production, mainly concentrated in the northern part of the eco-region at South-Central Chile (35° – 38° S, Lara et al. 2003).

According to the IPCC (Trenberth et al., 2007), South-Central Chile has experienced between 40 and 60% of decrease in precipitation in the period 1901–2005. In addition, increased water demands in the last decades have intensified problems in water availability (Lara et al. 2003). Due to the importance of Maule river for hydropower production and for agriculture in South-Central Chile, a streamflow reconstruction in this watershed is useful to assess last decades variations of water availability in a long term context and to better plan the future development of this part of the country.

2. Objectives

The main objective of this study is to develop a low-frequency streamflow reconstruction for the northern portion of the eco-region in the Mediterranean climate of South-Central Chile (35° – 36° 30'S), specifically for the Maule river watershed.

3. Methods

3.1 Study area

The study area corresponds to the Maule watershed in South-Central Chile (Figure 1). Climate in this area is of the Mediterranean type. Rain is concentrated in austral fall and winter (April–August), when over 75% of the annual precipitation occurs (Miller, 1976). Annual precipitation varies between approximately 830 mm in the coastal area and approximately 2300 mm in the Andes. According to the available stations, the mean January temperature corresponds to 19° C and the mean July temperature to 7.9° C (DGA).

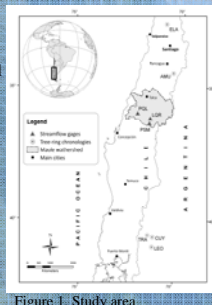


Figure 1. Study area

3.2 Streamflow records

To obtain the suitable streamflow data for the reconstruction, monthly values of the available streamflow records were divided by the mean of the 1965–2000 period, hence a percentage (%)/100 value was calculated for every month and for each station. Monthly correlations among stations were obtained for all the gages. According to this, only stations with significant correlation ($p < 0.95$) among each other every month, and with no anomalous patterns in monthly plots were selected as candidate records to be used in the reconstruction. After the selection of gages made to maximize the regional streamflow signal (three gages, Figure 1, Figure 2), several combinations of mean streamflow for different periods and seasons were calculated for each station. After this calculation, a new mean record was created by averaging the three selected stations (Figure 2). This new record with its respective seasons was used in the reconstruction process.

3.3. Chronologies

The tree-species selected for having the best correlations between tree-rings and streamflow in the area was *Austrocedrus chilensis*. Increment cores from living trees and cross-sections from dead trees were collected from two *Austrocedrus chilensis* stands in Central Chile and three stands in the Argentinean Patagonia (Figure 1). Samples were crossdated and standardized using conventional methods in dendrochronology that adjust to every individual tree-ring series a negative exponential curve or a linear regression. The mentioned chronologies were grouped into two composite chronologies, one for the northern sites and one for the southern ones (Figure 3). The sites' characteristics of each tree-ring chronology are described in Table 1.

3.4. Streamflow reconstruction

The growth of both *Austrocedrus* composite chronologies was correlated with monthly streamflow to see which were the months with the best correlation and to determine the period to be reconstructed (Figure 4 and 5). The reconstruction equation was estimated by regressing streamflow discharge on principal components (PCs) of the tree-ring composite chronologies best correlated with streamflow data (Figure 6 and 7). The quality of the regression model was assessed using the Pearson correlation coefficient (r), product mean test (t), and reduction of error statistic (RE , Table 2). The five lowest and highest annual streamflows in the reconstruction were also determined to see the distribution of these values along the centuries (Table 3). A Singular Spectral Analysis (SSA) was used to determine the dominant periods at which variance occurs in the streamflow reconstruction (Figure 8).

Pearson's temporal correlation coefficients between monthly and seasonal streamflow and indices of atmospheric circulation, such as the Antarctic Oscillation (AAO) and ENSO, were evaluated to identify the major climatic forcings affecting interannual variations in the Maule watershed discharge (Figure 9). Finally, sea surface temperatures (SST) were compared with the Maule streamflow to determine the atmospheric and oceanic features more closely related to streamflow variations in this watershed (Figure 10).

Table 1. Codes, location and elevation of the chronologies used in this study

Composite chronologies	Sites	Code	Location	Elevation (m)
ELA-AMU	El Asiento	ELA	$32^{\circ} 39' S$ - $70^{\circ} 49' W$	1700-1900
	Agua de la Muerte	AMU	$34^{\circ} 31' S$ - $70^{\circ} 25' W$	1700-2000
LE-CU-TR	Trafal	TRA	$40^{\circ} 39' S$ - $71^{\circ} 24' W$	1050
	Cuyin Manzano	CUY	$40^{\circ} 43' S$ - $71^{\circ} 08' W$	900
	Cerro Los Leones	LEO	$41^{\circ} 05' S$ - $71^{\circ} 09' W$	1020

4. Results

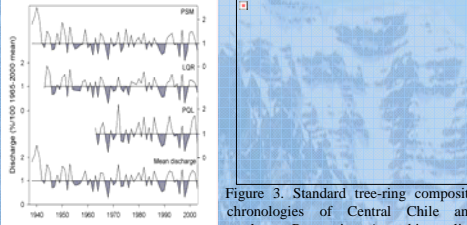


Figure 2. Annual streamflow discharge recorded at each of the selected gages, and the mean regional discharge calculated from averaging the three records.

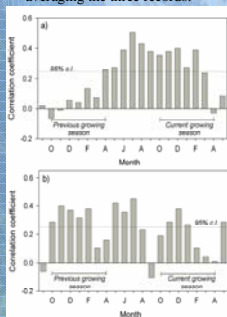


Figure 4. a) Correlations between monthly mean streamflow data at the Maule watershed and the northern composite chronology AMU-ELA b) as in a), but for the southern composite chronology LE-CU-TR.

4.1 Streamflow reconstruction

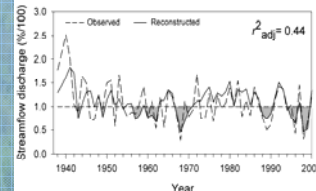


Figure 6. Observed and reconstructed mean annual (January to December) streamflow discharges for the Maule watershed streamflow from 1938 to 2001.

Table 2. Calibration and verification statistics computed for the tree-ring based reconstruction of annual streamflow.

Calibration	Verification
Time period	r^2 period
1938–1977	0.38
1962–2001	0.50
1938–2001	0.44

$$\text{Reconstruction Equation}$$

$$SFDr = 1.083 + 0.234PCIt$$

SFDr : Estimated streamflow discharge (%/100) for January to December of year t

PCIt : Principal component amplitude of the two composite chronologies for year t

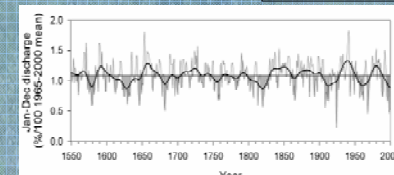


Figure 7. Annual streamflow reconstruction (January–December) of the Maule watershed for the 1550–2001 period.

Table 3. List of the five highest and lowest annual reconstructed streamflows.

Highest streamflows		Lowest streamflows	
Year	Mean discharge (%/100)	Year	Mean discharge (%/100)
1941	1.834	1924	0.224
1653	1.809	1968	0.459
1942	1.714	1998	0.463
1571	1.624	1982	0.501
1940	1.623	1999	0.519

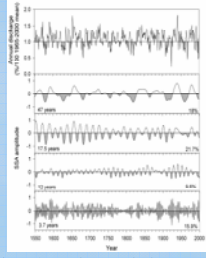


Figure 8. Maule watershed streamflow reconstruction (top) and its relation with the SOI, El Niño and La Niña events since 1950 are indicated as solid and dashed arrows, respectively, b) Summer–Fall streamflow and the AAO averaged for February–March.

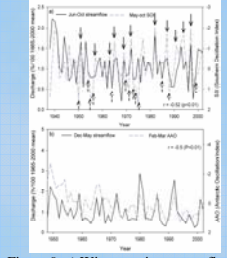


Figure 9. a) Winter–Spring streamflow and its relation with the SOI, El Niño and La Niña events since 1950 are indicated as solid and dashed arrows, respectively, b) Summer–Fall streamflow and the AAO averaged for February–March.

5. Discussion and conclusion

The present 450-year annual streamflow reconstruction constitutes the longest one developed in South America. This was built using the first principal component of two composite chronologies from the north (32° – 34° S) and south (40° – 41° S) of the study area. The fact that chronologies from these two areas are related to the Maule watershed streamflow, means that the precipitation regime in this watershed would be representing a transitional condition combining two different regimes: the one from Central Chile and the one from northern Patagonia. The regression model explained 44% of the total variance in the annual streamflow. In reference to the lowest streamflows, four of the five lowest streamflows years in the last 450 years are in the 20th century reflecting more severe drier conditions in the last century compared to previous ones. The most important oscillation mode in terms of explained variance corresponds to the interdecadal oscillation with a periodicity of about 17.5 years. This signal is especially strong before the 20th century (Figure 8). According to Villalba et al., (2001), this is a common pattern to several proxy records across the Pacific basin, suggesting that interdecadal variations in the Pacific-related climate system were more noticeable before the 20th century. The second most important oscillation corresponds to the 47-year cycle, which is especially important since the second half of the 19th century (Figure 8). Explanations for this cycle might be the half-Gleisberg solar magnetic cycle or possibly the Pacific Decadal Oscillation that presents an approximate cycle of around 50 years in a tree-ring reconstruction for the past Millennium (MacDonald and Case, 2005). Correlations between the Maule watershed streamflow and climatic forcings indicate that streamflow in this area is influenced by climatic features of both low and high latitudes. Winter–spring streamflow is significantly influenced by ENSO, and summer–fall by the AAO, being stronger the relationship with ENSO. The positive projected trend for the AAO might bring drier conditions to midlatitudes and likely have an effect on the Maule watershed streamflow. However, this influence is certainly weaker than the one that the AAO exerts over streamflows further south where the negative trend is more pronounced (Lara et al., 2008). This reconstruction provides valuable information for decision makers in water resources planning, especially in a watershed characterized by intensive agricultural and hydroelectric use and under an existing climate change and intensification of water use scenario.

6. References

- Arnell N. et al. (2001) Hydrology and water resources. In: IPCC. Climate Change 2001. Impacts, adaptation and vulnerability. Cambridge University Press, Cambridge, pp 193–233 (Chapter 4)
- Cook R. and K. Peters (1981) The smoothing spline: a new approach to standardizing forest interior ring-width series for dendroclimatic studies. Tree-Ring Bulletin, 11:45–53.
- Fritts H.C. (1976) Tree rings and climate. Academic, London, p. 567.
- Lara, A., Soto, D., Arnesto, J., Donoso, P., Werner, C., Nahuelhual, L. and Siqueo, F. (eds.) (2003) Componentes científicos clave para una política nacional sobre usos, servicios y conservación de los bosques nativos Chilenos. Universidad Austral de Chile. Iniciativa Científica Milenio de Mideplan, p. 134.
- Lara, A., Villalba, R., and Urrutia, R. (2008) A 400-year tree-ring record of the Puelo River summer–fall streamflow in the Valdivian rainforest eco-region, Chile. Climatic Change, doi:10.1007/s10584-007-9287-7. Vol 86 (3–4):331–356.
- MacDonald G., and R. Case (2005) Variations in the Pacific Decadal Oscillation over the past millennium. Geophysical Research Letters 32 L07203, doi:10.1029/2004GL022478.
- Miller, A. (1976) The Climate of Chile. In: Schwerdtfeger, W. (ed.), World Survey of Climatology. Climates of Central and South America. Elsevier, Amsterdam, The Netherlands, pp.113–131.
- Trenberth, K.E., P.D. Jones, P. Ambenje, R. Bojanini, D. Easterling, A. Klein Tank, D. Parker, F.Rahmstorf, J.A. Renwick, M. Rusticucci, B. Soden and Zhai, P. (2007) Observations: Surface and Atmospheric Climate Change. In: Climate Change 2007: The Physical Science Basis. Contribution of Working Group I to the Fourth Assessment Report of the IPCC. Cambridge University Press/Cambridge, United Kingdom and New York.
- Villalba, R., D. Arango, R. Cook, E. Wiles, G. Jacoby, G.C. (2001) Decadal-Scale Climatic Variability along the Extratropical Western Coast of the Americas: Evidences from Tree-Ring Records. In: Margraf V. (ed.), Interhemispheric Climate Linkages. Academic Press, San Diego, California, U.S.A., pp.155–172.